

Effects of ventilator configuration on the flow pattern of a naturally-ventilated three-span Mediterranean greenhouse

Karlos Espinoza, Alejandro López, Diego L. Valera*, Francisco D. Molina-Aiz, José A. Torres, Araceli Peña

Research Centre on Mediterranean Intensive Agrosystems and Agrifood Biotechnology (CIAIMBITAL), University of Almería, Ctra. Sacramento s/n, 04120 Almería, Spain

Abstract

Natural ventilation used in agricultural greenhouses is important to control greenhouse microclimate. The effect of the ventilator configuration on the flow pattern of a three-span Mediterranean greenhouse with an obstacle to airflow (a neighbouring greenhouse) was investigated. Two different ventilator configurations, two or three half-arch roof vents with two roll-up side vents, were evaluated using sonic anemometry. It was observed that the flow pattern through the greenhouse depends of the ventilation surfaces distribution and the obstruction to the ventilation system. Moreover, the magnitude and distribution of ventilation surface affected the overall ventilation rate and the ventilation rate at plant level. The ventilator configuration with two roof and two side vents improved air movement at the plant level, although the overall volumetric flow rate was lower than that with three roof and two side vents.

Keywords: Ventilation, Airflow, Sonic Anemometry

1. Introduction

Almería in Spain with its warm climate (3,000 h yr⁻¹ of sunshine) and extensive area of protected cropping (> 30,000 ha) (Valera, Belmonte, Molina-Aiz, and López, 2016) is representative of the 700,000 ha worldwide of protected cropping (Katz and Weaver, 2003). Agricultural production in the greenhouses in this region requires

*Corresponding author. Tel.: +34-950-015-546; Fax: +34-950-015-491

Email addresses: ker154@ual.es (Karlos Espinoza), alexlopez@ual.es (Alejandro López), dvalera@ual.es (Diego L. Valera), fmolina@ual.es (Francisco D. Molina-Aiz), jtorres@ual.es (José A. Torres), apfernan@ual.es (Araceli Peña)

Preprint submitted to Biosystems Engineering

August 25, 2017

Nomenclature

Acronyms

<i>E</i>	Relative measurement error of the flow rate, [%].
<i>F</i>	Pressure drop coefficient.
<i>G</i>	Volumetric flow rate, [m ³ s ⁻¹].
<i>K</i>	Permeability, [m ²].
<i>N</i>	Hourly volumetric air exchange rate, [h ⁻¹].
<i>NS</i>	Number of samples.
<i>OR</i>	Inlet-to-outlet opening ratio.
<i>Ph</i>	Plant height, [cm].
<i>S</i>	Surface area, [m ²].
<i>T</i>	Temperature of the air, [°C].
<i>t</i>	Time, [s].
<i>Tn</i>	Test number.
<i>Ts</i>	Sonic temperature, [°C].
<i>U</i>	Wind speed, [m s ⁻¹].
<i>u</i>	Air velocity, [m s ⁻¹].
<i>V</i>	Volume, [m ³].
<i>VX</i>	Vent number <i>X</i> .
<i>Y</i>	Inertial factor.

Symbols

η	Transport efficiency coefficient.
ψ	Side-roof vents flow rate ratio.

φ	Porosity, [%].
ϑ	Roof and side opening surface ratio.
ξ	Wind and thermal forces ratio, [m ^{°C} ^{-0.5} s ⁻¹].

Subscripts

Θ	True north-based azimuth, [°].
<i>c</i>	Corrected measure.
<i>g</i>	Greenhouse.
<i>i</i>	Inside.
<i>io</i>	Outlet.
<i>j</i>	Elementary sample.
<i>l</i>	Leeward.
<i>ne</i>	Northeast direction.
<i>o</i>	Outside.
<i>oi</i>	Inlet.
<i>p</i>	Porous medium.
<i>r</i>	Roof.
<i>s</i>	Side.
<i>sw</i>	Southwest direction.
<i>v</i>	Vent(s).
<i>w</i>	Windward.
<i>x</i>	Component on the <i>x</i> direction on the coordinate plane.

control of excessively high temperatures. The aim is to achieve this control with systems that consume less energy and have less environmental impact (Valera et al., 2016). To control temperatures nearly all farmers in Almería whiten greenhouse covers and use natural ventilation, with side and roof vents having an average ventilation surface of 14.4% being commonly used (Valera et al., 2016).

Natural ventilation is a simple system that is energy-friendly, low-cost and requires little maintenance. The process allows the exchange of energy and mass between the external environment and the interior of the greenhouse (Boulard, Lamrani, Roy, Jaffrin, and Bourden, 1998); thus, the system has a strong influence on the greenhouse microclimate. For these reasons, natural ventilation is widely used in Almería to control air temperature, humidity, and gas concentrations for most of the cropping cycle. Controlling the microclimate parameters leads to enhancement of the photosynthetic and transpiration processes of plants, and yield can be improved (Max, Horst, Mutwiwa, and Tantau, 2009).

The air exchange that occurs mainly through greenhouse openings as a consequence of temperature and pressure variations between the interior and exterior of the greenhouse is defined as natural ventilation. The main driving forces in the process are buoyancy and convection associated with wind (Kittas, Boulard, and Papadakis, 1997) and they contribute to the flow pattern in the greenhouse. When the wind speed is low, buoyancy forces induce an upward flow displacement and this can be observed as air circulation inside the greenhouse. Ventilation rate and flow pattern have also been attributed to wind intensity (Bot, 1983). Boulard, Foulloley and Kittas (1997) observed that wind intensity has a linear dependence on the air exchange rate when buoyancy is disregarded. In order to determine when these forces assist or oppose each other, the ratio of buoyancy and wind forces is used (Li and Delsante, 2001).

Studies have shown that not only is wind intensity important in the ventilation process, but ventilation rates (Hong et al., 2008; Shklyar and Arbel, 2004), flow pattern (Boulard, Meneses, Mermier, and Papadakis, 1996; Teitel, Ziskind, Liran, Dubovsky, and Letan, 2008), and the microclimate (Bartzanas, Boulard, and Kittas, 2002; Roy and Boulard, 2005) inside the greenhouse also depend on the wind direction. Moreover, the natural ventilation process alters the air velocity (Bartzanas et al., 2002; Molina-Aiz, Valera, and Álvarez, 2004), temperature, and humidity (Molina-Aiz et al., 2004; Teitel, Liran, Tanny, and Barak, 2008; Teitel, Ziskind, et

al., 2008) gradients within the greenhouse, which could affect crop development (Majdoubi, Boulard, Fatnassi, and Bouirden, 2009).

Crop within the greenhouse also contributes to the flow pattern inside the greenhouse (Majdoubi et al., 2009; Molina-Aiz, Valera, Álvarez, and Madueño, 2006; Molina-Aiz, Valera, Peña, and Gil, 2005) and greenhouse design parameters play an important role in the ventilation process. Several studies have confirmed that there is a decay relationship between the ventilation rate and the number of spans in a greenhouse (Esteban J Baeza et al., 2009; Kaçira, Sase, and Okushima, 2004a; Kaçira, Short, and Stowell, 1998; Lee et al., 2003; Molina-Aiz et al., 2005). This relationship also seems to depend on roof geometry (Perén, Van Hooff, Leite, and Blocken, 2016; Perén, Van Hooff, Ramponi, Blocken, and Leite, 2015).

The type of vent used in the greenhouse also affects ventilation efficiency (Bartzanas, Boulard, and Kittas, 2004; Kittas, Boulard, Mermier, and Papadakis, 1996; Molina-Aiz and Valera, 2011). Insect-proof screens installed in vents reduce the inlet airspeed and ventilation rate, resulting in higher temperature and humidity within the greenhouse (Esteban J Baeza et al., 2009; Bartzanas et al., 2002; Campen and Bot, 2003; Fatnassi, Boulard, Demrati, Bouirden, and Sappe, 2002; Harmanto, Tantau, and Salokhe, 2006; Katsoulas, Bartzanas, Boulard, Mermier, and Kittas, 2006; Molina-Aiz et al., 2004; Teitel, 2001).

Vent configuration, position, and dimensions also have a strong effect on flow pattern and ventilation rate. The use of side vents, and their size, influences ventilation rate, affecting the temperature distribution within the greenhouse (Bartzanas et al., 2004; Molina-Aiz and Valera, 2011; Short and Lee, 2002). Similarly, Baeza, Pérez Parra and Montero (2005) observed in a '*parral*' (Almería) greenhouse that has larger roof vents that can improve ventilation. The ratio between the open area of a roof and the area of the side vents and the ground area have been used to describe the quality of the ventilation system relative to the ground area covered (Kittas et al., 1997). Notwithstanding this, there are additional parameters that affect the ventilation process. The vertical location of the side vent has an influence on the temperature distribution and the ventilation rate (Bournet, Ould Khaoua, and Boulard, 2007; Bournet, Ould Khaoua, Boulard, Migeon, and Chassériaux, 2007; Molina-Aiz and Valera, 2011; Short and Lee, 2002), whereas the height difference between the roof and the side vent affects the flow pattern (Bournet and Boulard, 2010), but it has a minimal influence on the velocity of the occupied zone (Perén, Van Hooff, Leite, and Blocken, 2015). In addition, there are several suggestions as

to how vents should be oriented. The optimal roof vent orientation seems to depend on the use of side vents. Kaçira, Short and Stowell (1998); Baeza, Pérez and Montero (2009); López (2011); Molina-Aiz and Valera (2011) found that a combination of side vents and roof vents oriented to leeward improved ventilation capacity of a greenhouse, while Ould Khaoua, Bournet, Migeon, Boulard and Chassériaux (2006) observed that for a glass greenhouse with only roof vents, the ventilation rate was significantly enhanced by orienting the roof vents windward. However, these glass greenhouses are less influenced by wind direction, due to the effect of roof openings (Hong et al., 2008). When side ventilation is used, the inlet-to-outlet opening ratio has an important effect on the volume airflow rate (Perén et al., 2016).

The aim of this study is to improve the understanding of the effects of the ventilator configuration on the flow pattern in a full-size multi-span greenhouse. This work also intends to provide a thorough understanding of the flow pattern developed when the ventilation system in the green house is exposed to two wind directions and a low and high wind speed when configured with four and five open vents (two side vents in combination with two or three roof vents).

2. Materials and methods

2.1. Experimental greenhouse and crop

An experiment was performed in a three-span Mediterranean greenhouse (Fig. 1) located at the agricultural research farm 'Eduardo Fernández' of the University of Almería, Spain (36°51'52.4 N, 2°16'58.5" W, 87 m above sea level), with the ridge of the greenhouse oriented 118° azimuth. A polyethylene sheet separated the greenhouse into two compartments, allowing us to study the western compartment, which has less wind obstruction (López, Valera, and Molina-Aiz, 2011). The western side of the greenhouse had a surface S_g of 480.0 m² and a volume V_g of 2,499.7 m³ with the roof vents closed. Each roof vent had a volume of 79.8 m³ when they were open.

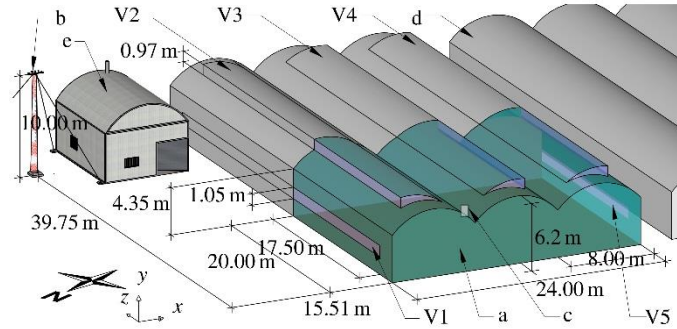


Fig. 1: Experimental greenhouse. Western half of the experimental greenhouse (a); weather station (b); temperature and humidity sensor (c); neighbouring greenhouse (d); warehouse (e); side vents (V1 and V5); and roof vents (V2, V3, and V4).

Inside the greenhouse, a tomato crop (*Lycopersicon esculentum* L. ‘Marenza’) was grown in rows oriented 28° azimuth, perpendicular to the vent and parallel to the interior main air flow, was observed in a previous work (López, Valera, Molina-Aiz, and Peña, 2012). During the experiment, crop height, number of leaves, and leaf area index were measured to observe the influence of the crop on the flow pattern in the greenhouse.

2.2. Equipment and instruments

External environmental conditions were measured at a height of 10 m (Fig. 1, b) by a meteorological station composed of three sensors (Hortimax S.L., Spain). MeteoStation II measured windspeed and direction using a cup anemometer (measurement range 0 m s⁻¹ to 40 m s⁻¹; accuracy ±5%; resolution 0.01 m s⁻¹) and a vane sensor (measurement range 0° to 360°; accuracy ±5%; resolution 1°), respectively. A Butron II (Hortimax S.L., Spain) measured temperature with a Pt100 temperature sensor (measurement range -25 °C to 75 °C; accuracy ±0.01 °C) and humidity with a capacitive humidity sensor (measurement range 0% to 100%; accuracy ±3%). Solar radiation was measured with a Solari (Hortimax S.L., Spain) sensor (measurement range 0 W m⁻² to 2.000 W m⁻²; accuracy ±20 W m⁻²). Inside the greenhouse, temperature and humidity were measured at a height of 2 m (Fig. 1 c) by an Ektron II-C sensor (Hortimax S.L., Spain). It was composed of a Pt100 temperature sensor (measurement range -10 °C to 60 °C; accuracy ±0.6 °C) and a capacitive humidity sensor

(measurement range 0% to 100%; accuracy $\pm 3\%$). Both the external and internal microclimate variables were recorded at a frequency of 0.5 Hz by a MultiMa Series II controller-datalogger (Hortimax S.L., Spain).

In order to measure the air velocity, direction, and temperature of the flow through the vents of the greenhouse, two CSAT3 3D sonic anemometers were used (Campbell Scientific Spain S.L., Spain; measurement range 0 m s^{-1} to 30 m s^{-1} and -30 °C to 50 °C; accuracy ± 0.04 m s^{-1} and ± 0.026 °C; resolution 0.001 m s^{-1} and 0.002 °C) and 10 Windsonic 2D sonic anemometers (Gill Instrument Ltd, UK; measurement range 0 m s^{-1} to 60 m s^{-1} ; accuracy $\pm 2\%$; resolution 0.01 m s^{-1}). These variables were recorded with a frequency of 10.0 Hz for the 3D sonic anemometers and 1.0 Hz for the 2D sonic anemometers by two CR3000 dataloggers (Campbell Scientific Spain S.L., Spain).

2.3. Ventilation system

The ventilation system of the greenhouse (Fig. 1) was composed of two continuous roll-up side vents (V1 and V5) (each vent had a size $S_s = 1.05 \text{ m} \times 17.5 \text{ m}$, was oriented 118° azimuth, and had an opening angle of 90°), and three continuous half arch roof vents (V2, V3, and V4) (each vent had a size $S_r = 0.97 \text{ m} \times 17.5 \text{ m}$, was oriented 118° azimuth, and had an opening angle of 14°). Roof vent V2 faced the east wind, while the other two roof vents, V3 and V4, faced the west wind. The height difference between the roof and side vents was 4.11 m.

Insect-proof screens made of high-density polyethylene were installed on each greenhouse vent. In the side openings, the screens were set tight against the structure, but in the roof openings, the screens were more loosely installed. This is a common installation practice in roof openings that work with a mechanical system in order to avoid damage from over straining the insect-proof screens. The geometric characteristics of the insect-proof screens, estimated using the methodology and image processing algorithm proposed in previous studies (Álvarez, Oliva, and Valera, 2012; López, Valera, Molina-Aiz, Peña, and Marín, 2013; Valera et al., 2005), included: porosity $\varphi_m = 26.3\%$, pore length in the weft (110.0 μm) and warp (611.9 μm) direction,

diameter of the thread in the weft (187.7 μm) and warp (209.4 μm) direction, diameter of the inside circumference of the pore (113.5 μm), area of the pore (0.067 mm^2), and thickness (458.1 μm). The aerodynamic parameters of the insect-proof screens were determined with the method proposed by Miguel, Van De Braak and Bot (1997) using a subsonic wind tunnel system developed by Valera, Álvarez and Molina-Aiz (2006) and Espinoza, Valera, Torres and Molina-Aiz (2015); permeability $K_p = 1.22 \times 10^{-9} \text{ m}^2$, inertial factor $Y = 0.239$, and pressure drop coefficient $F_\varphi = 26.29(0.239 + Re^{-1})$.

2.4. Test setup

Two different ventilation system configurations, A and B, were evaluated (Fig. 2). In both configurations, side vents (V1 and V5) were opened, resulting in a side ventilation surface S_s of 36.8 m^2 .

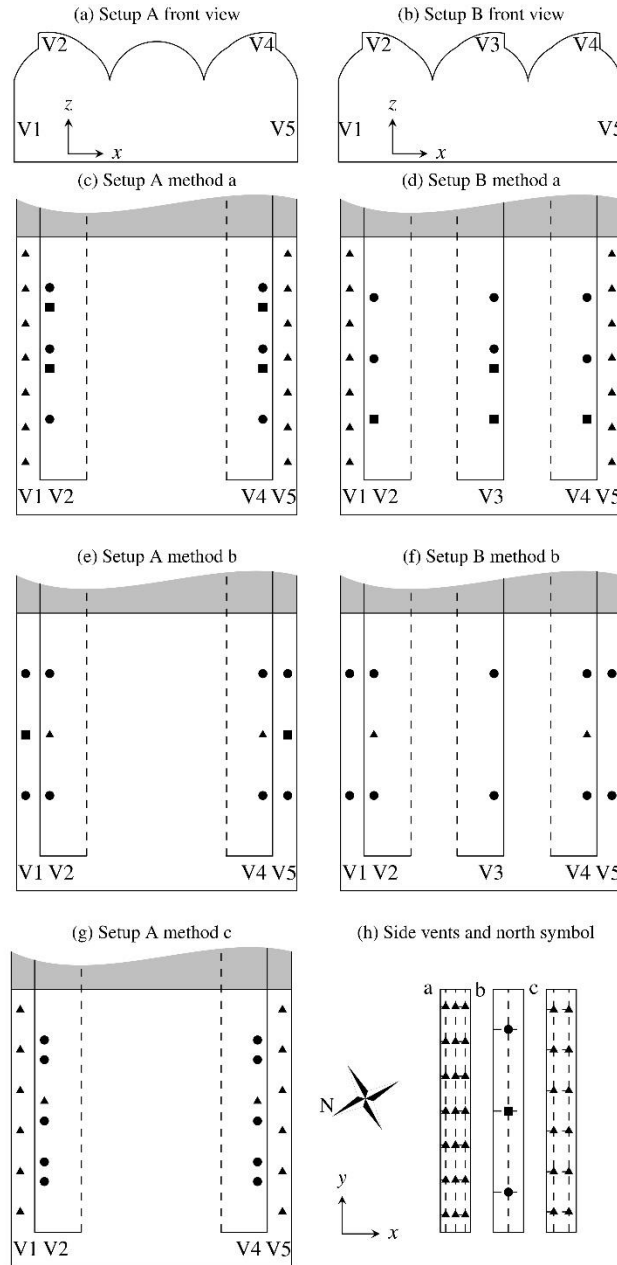


Fig. 2: Sonic anemometer sampling location layout for each setup and sampling methodology. Front view (vertical plane XZ) of ventilator configuration using two open roof vents (setup A) and three open roof vents (setup B) (subfigures a and b, respectively). Top view (horizontal plane XY) of sensor sampling location layout for setup A using methods (a), (b), and (c) (subfigures c, e, and g, respectively) and for setup B using methods (a) and (b) (subfigures d and f, respectively). Front view (vertical plane YZ) of sensor sampling location layout at side vents (V1 and V5) using measuring methods (a), (b), and (c) (subfigure h). 3D sonic anemometer (\blacktriangle); 2D sonic anemometer measuring horizontal plane XY (\bullet); 2D sonic anemometer measuring vertical plane XZ (\blacksquare).

When the greenhouse was configured with setup A, two roof vents were opened (V2 and V4). With this

configuration, roof ventilation surface S_r was 33.9 m², total ventilation surface $S_{r,s}$ was 70.7 m², ventilation surface ratio $S_{r,s}/S_g$ was 17.4%, and the greenhouse volume was 2,659.3 m³.

Considering windward vents as the inlet openings and leeward vents as the outlet openings, the inlet-to-outlet opening ratio (Perén et al., 2016) was the same for both wind directions (from northeast and southwest):

$OR_{ne,sw} = S_w/S_l = 1.00$. In order to determine the effect of the windward and leeward openings, the roof and side opening surface ratio ϑ was estimated as:

$$\vartheta_w = \frac{S_{w,r}}{S_{w,s}}, \vartheta_l = \frac{S_{l,r}}{S_{l,s}} \quad (1)$$

where S_r was the roof vent and S_s was the side vent in the windward w or leeward l side. Thus, for setup A, $\vartheta_{ne,sw}$ was 0.92 for both wind directions, northeast and southwest.

When the greenhouse was configured with setup B, all vents (V1 to V5) were opened. With this configuration, the ventilation surface and volume characteristics were as follows: roof surface ventilation $S_r = 50.9$ m², total ventilation surface $S_{r,s} = 87.7$ m², surface ventilation ratio $S_{r,s}/S_g = 18.3\%$, and the greenhouse volume $V_g = 2,739.1$ m³. The inlet-to-outlet opening ratio was $OR_{ne} = 0.68$ and $OR_{sw} = 1.48$ for wind from the northeast and southwest, respectively. The roof and side opening surface ratio $\vartheta_{V3V4,V5}$ was 1.85 for roof vents V3, V4 with side vent V5 and $\vartheta_{V2,V1}$ was 0.92 for roof vent V2 and width vent V1.

In order to determine the best method to measure the airflow using the limited number of sonic anemometers, three different sampling methods were carried out (Fig. 2). Method (a) consisted of 21 samples (3 min per sample), homogeneously distributed in each side vent, were measured during the test period (2 h) by a mobile 3D sonic anemometer and 10 2D sonic anemometers fixed at the roof vents. Method (b) used one 3D sonic anemometer per roof vent that was fixed at the middle of the vent surface during the 4 h test period. Method (c) used a 3D sonic anemometer for both side vents, measuring 12 samples (3 min per sample) per vent, and the other 3D sonic anemometer was used to measure one sample (15 min per sample) per roof vent during the 2 h test period. For all measuring methods (a, b, and c), 2D sonic anemometers were in a fixed position during the tests, with different orientations to measure air flow in both planes, the horizontal plane XY and the vertical plane XZ . With these layout, the average ventilation surface corresponding to each sampling point, named as

sample surface, was estimated using:

$$\bar{S}_{v,j} = \frac{S_v}{NS_v} \quad (2)$$

where NS is the number of sampling points. The sample surface for each setup and measuring method is indicated in [Table 1](#) and was based on that used in a previous study (López, 2011; López et al., 2012).

Table 1: Test repetitions and sample surface per measuring method. Test time duration Td [min]; sample surface for the side vents $\bar{S}_{v1,v5,j}$, the central roof vent $\bar{S}_{v3,j}$, and north and south roof vents $\bar{S}_{v2,v4,j}$ [$\text{m}^2 \text{point}^{-1}$]. See supplementary material [Table B1](#) for detailed time information of each repetition.

Setup	Measuring method	Repetitions	Td	$\bar{S}_{v1,v5,j}$	$\bar{S}_{v3,j}$	$\bar{S}_{v2,v4,j}$
A	a	6	89–109	0.88	–	3.40
	b	11	420–450	6.13	–	5.66
	c	6	114–141	1.53	–	2.83
B	a	7	90–213	0.88	4.24	5.66
	b	8	420–420	9.19	8.49	5.66

With the same greenhouse it was found that the directions of the velocity vectors were similar across the interior of the greenhouse at three different heights (1.00 m, 1.75 m and 2.50 m), and that the average crop height in this study was 146.22 cm (plus 20 cm of the plant pot height), measurement points in side vents were used to describe the flow at crop level.

A simple ANOVA analysis using Statgraphics Centurion XVI (StatPoint Technologies, USA) was performed to determine the performance of each method by analysing the error in the ventilation rate $E_{\bar{G}}$ between sampling methodologies. This error was estimated using the expression (López, Valera, Molina-Aiz, and Peña, 2011; Molina-Aiz, Valera, Peña, Gil, and López, 2009):

$$E_{\bar{G}} = \frac{G_{oi} - G_{io}}{\bar{G}} 100 \quad (3)$$

where $G = (G_{oi} + G_{io})/2$ is the mean ventilation rate.

2.5. Ventilation process analysis

This study focused on how the flow pattern is affected by the vent arrangement of a greenhouse. Tests were

grouped by low and high wind speed. These groups were then classified by northeast wind ($U_{o,\theta} \in [332^\circ, 118^\circ]$ azimuth) and southwest wind ($U_{o,\theta} \in [118^\circ, 332^\circ]$ azimuth). The flow pattern comparison between the test setups of each group was performed by selecting the tests with the most similar wind speed and air temperature difference between the interior and exterior of the greenhouse. This task was achieved using both parameters of each test to calculate the Euclidean distance, and the test setups with the shortest distance were selected.

The flow pattern for each test was visualised by calculating the mean velocity vector for each sample location at the vents. The frequency distribution of the flow was observed by estimating the polar histograms of each calculated velocity vector as in the studies by Wang and Deltour (1997, 1999a, 1999b). The vector arrows and histograms were drawn using relative spatial positions. This allowed the flow pattern for each test in both planes to be analysed; the horizontal plane XY , and vertical plane XZ .

Mean air velocity perpendicular to an opening was estimated with the x component of the measured air velocity vector. The other components (y and z) were neglected, as the contribution to the flow of the components that are not perpendicular to the opening is very small. This effect is more predominant as vent size increases (Van Overbeke, De Vogeleer, Brusselman, Pieters, and Demeyer, 2015). The mean flow velocity was calculated by (Cebeci, 2004):

$$u = \int_t^{t+\Delta t} u(t) dt \quad (4)$$

where $u(t)$ was the instantaneous air velocity (Heber, Boon, and Peugh, 1996) and Δt was the sample time previously described for each measuring method. In order to address the changing external conditions over the test period when using the measuring methods (a) and (c), only the flow measurement samples of the 3D sonic anemometers $u_{i,j}(t)$ were corrected using the average windspeed of the test period U_o and the sampling period $U_o(t)$ using (Boulard, Wang, and Haxaire, 2000; Molina-Aiz et al., 2009):

$$u_{i,j}^c(t) = u_{i,j}(t) \frac{U_o}{U_o(t)} \quad (5)$$

In order to describe the air circulation through all the openings, the corrected volumetric flow rate G was calculated for each elementary ventilation surface $S_{v,j}$, using its corresponding perpendicular air velocity

component $u_{x,j}$. Thus, the volumetric flow rate for each opening was (Boulard, Kittas, Papadakis, and Mermier, 1998; Molina-Aiz et al., 2009):

$$G = \sum_{j=1}^n S_{v,j} u_{x,j} \quad (6)$$

where n is the number of sampling locations per vent (see Table 1). The accuracy of the sampling strategy was assessed by the relative ventilation rate measurement error (Van Buggenhout et al., 2009; Van Overbeke et al., 2015; Van Overbeke, De Vogeleer, Pieters, and Demeyer, 2014; Van Overbeke, Pieters, De Vogeleer, and Demeyer, 2014).

$$E_{G_{oi}} = \frac{G_{oi} - G_{io}}{G_{oi}} 100 \quad (7)$$

In order to reduce error caused by the influence of entrained and recirculating air, the inlet volumetric flow rate G_{oi} , which has a greater normal-to-opening component, was considered the reference ventilation rate. The volumetric air exchange per hour was assessed by the rate (Bot, 1983):

$$N = 3,600sh^{-1} \frac{G}{V_g} \quad (8)$$

where V_g is the greenhouse volume, including the volume of the open vents. The exchange rate was estimated for both \bar{G} and G_{oi} .

The flow rate pattern through the ventilator configuration was analysed by calculating the percentage of the inlet $Q_{oi,VX}\%$ and outlet $Q_{io,VX}\%$ flow rate through each vent. Additionally, the ratio ψ of the flow rate percentage through the side vent $Q_{s,VX}\%$ and the flow rate percentage through the roof vents $Q_{r,VX}\%$ with the same opening orientation was estimated by:

$$\psi = \frac{Q_{s,VX}\%}{Q_{r,VX}\%} \quad (9)$$

The side-roof vents flow rate ratio was estimated for the openings oriented toward the northeast (side vent V1 and roof vent V2) and for the openings oriented toward the southwest (side vent V5 and roof vents V3 and V4).

One of the main processes encompassed by natural ventilation is the exchange of energy between the interior

and the exterior of the greenhouse. Thermal energy exchange efficiency was estimated with the coefficient (Tanny, Haslavsky, and Teitel, 2008):

$$\eta_T = \frac{T_i - T_o}{\Delta T_{i,o}} \quad (10)$$

where inside T_i and outside T_o air temperature were measured with the Ektron II-C sensor and the meteorological station. The outlet temperature T_{io} and the air temperature difference $\Delta T_{i,o}$ were calculated.

The outlet temperature was measured with the 3D sonic anemometers and corrected with the method described by Sozzi and Favaron (1996) and then normalized with the model proposed by López, Valera, Molina-Aiz and Peña (2011). Therefore, T_{io} could only be recorded in the vents where there was an outlet flow and a 3D sonic anemometer. This difference in thermal energy induces buoyancy forces, but there is also a wind force over the flow in the greenhouse. A parameter that describes this relation is the wind-thermal forces ratio, calculated as (Kittas et al., 1997):

$$\xi = \frac{U_o}{\sqrt{\Delta T_{i,o}}} \quad (11)$$

3. Results and discussion

3.1. Analysis of the sampling methods

Based on the estimated error in the ventilation rate (Eq. (3)), the three sampling methods, (a), (b), and (c), two and three open roof vents (setups A and B), did not differ significantly vary in terms of reducing the error in the ventilation rate at a confidence level of 95% ($p > 0.05$) in accordance with Fisher's least insignificant difference procedure. Nevertheless, a greater resolution of the velocity vector field was obtained with methodologies (a) and (c), in which a greater number of sampling locations were used at each vent. Also, sampling method (c) allows inlet/outlet flow temperature on both side and roof vents to be measured. This method achieved an average sample surface of $2.18 \text{ m}^2 \text{ point}^{-1}$, similar to the $2.10 \text{ m}^2 \text{ point}^{-1}$ and $2.60 \text{ m}^2 \text{ point}^{-1}$ used by Molina-Aiz, Valera, Peña, Gil and López (2009) and Boulard, Kittas, Papadaskis and Mermier (1998), respectively. Better estimation of the ventilation rate could be achieved by reducing this sample surface, as in the sampling method of Van Overbeke, De Vogeleeer, Brusselman, Pieters and Demeye

(2015) where the sample surface was $0.06 \text{ m}^2 \text{ point}^{-1}$ and an automatic sensor frame (Van Overbeke, De Vogelee, et al., 2014) with an opening of 0.5 m^2 was used. However, the simplest sampling method was method (b). With method (b) correction of measured samples was avoided, but spatial resolution was reduced. In the vast majority of replicated measurements (supplementary material [Table A1](#)) the perpendicular-to-vent component of the air velocity vector $u_{i,x}$ was greater for inlet flow rate than for outlet flow rate. As consequence, the calculated inlet flow rate Q_{oi} was greater than the outlet flow rate Q_{io} . Van Overbeke et al. (2015) also measured this difference in the normal components of two vents in a pig house. Moreover, the inlet flow tend to be normal to the opening. These patterns correspond to the formation downstream of the opening of an air jet, as observed in previous experiments (Bartzanas et al., 2004; Perén et al., 2016; Perén, Van Hooff, Leite, et al., 2015; Subudhi, Sreenivas, and Arakeri, 2013). This normal property of the inlet flow was used to reduce the error because the influence of entrained and recirculation of the airflow. Thus, this inlet flow was used as a reference to measure the error in the ventilation rate $E_{G_{oi}}$ (supplementary material [Table A1](#)).

3.2. Analysis of the flow pattern

The measured flow vectors (supplementary material [Figs. C1a to C13b](#)) allowed us to observe the flow pattern developed when using the two different vent configurations (two and three open roof vents). A discussion of the effect of the windspeed on the flow pattern for the different vent configurations is presented here for low and high wind speeds. $U_o = 4.00 \text{ m s}^{-1}$ and $\xi = 2.3 \text{ m}^{\circ}\text{C}^{-0.5}\text{s}^{-1}$ were used as threshold to describe the observed patterns for low and high wind speed. Additionally, an analysis of the transition from low to high, and the effect of the obstruction (the neighbouring greenhouse) is presented.

3.2.1. Low and high wind speed

The following sections present and discuss the observed flow rate pattern and air velocity vectors. Additionally, air streamlines deduced from the observed flow rate for each opening are discussed. In order to infer the streamlines in the greenhouse, the percentage of the flow rate per vent was calculated independently

for the inlet and outlet flow rate. Based on estimated flowrate percentages, the streamlines tended to rise because of buoyancy and tended to escape through the nearest roof opening causing a “short-circuit” (Norton, Grant, Fallon, and Sun, 2009). Thus, only the remaining inlet flow escaped through the side vent.

It was observed that a common flow pattern occurred in the 19 test repetitions (supplementary material [Figs. C1a to C13b](#)) when the greenhouse was ventilated with low windspeed ($U_o \leq 4.00 \text{ m s}^{-1}$ and $\xi \leq 2.3 \text{ m}^\circ\text{C}^{-0.5}\text{s}^{-1}$) and 18 test repetitions when the greenhouse was ventilated with high windspeeds ($U_o > 4.00 \text{ m s}^{-1}$ and $\xi > 2.3 \text{ m}^\circ\text{C}^{-0.5}\text{s}^{-1}$). A quantitative and a qualitative comparison between both ventilator configurations (setup A and B) ventilated with both wind directions is presented in this section using two tests: one test per setup type with the most similar wind and temperature conditions ([Figs. 3 and 4](#)).

Flow through the greenhouse was mostly driven by thermal forces when the greenhouse was exposed to low windspeeds. Thermal forces assisted the wind force in the windward side vent and roof leeward vents, but it opposed the wind in the windward roof vents and leeward side vent. Air direction polar histograms allowed us to observe this interaction. Where these forces assisted each other a high frequency was found in flow direction. However, when they opposed each other the air direction frequency was more disperse. Other studies (Esteban J Baeza et al., 2009; Kaçira et al., 1998; López, 2011; Molina-Aiz and Valera, 2011; Perén et al., 2016) have reported positive and negative (Kaçira, Sase, and Okushima, 2004b; Li and Delsante, 2001) interactions between wind and thermal forces in naturally ventilated buildings. Because of this interaction, the main flow moved from the windward side vent to the leeward roof vents for both ventilator configurations ([Figs. 3b, 3d, 3f and 3h](#)). Thus, the inlet flow rate of the windward side vent was on average 3.7 greater than the inlet flowrate of the windward roof vent with a northeast wind for both vents configurations. However, with a southwest wind only two open roof vents configuration (setup A) caused an inlet flow through the windward side vent.

In contrast, the flow pattern was mostly driven by wind forces when the greenhouse was ventilated with high wind speed ([Figs. 4b, 4d, 4f and 4h](#)). Under this condition, vector directions were mostly driven by vent configuration, greenhouse geometry and the obstruction (neighbouring greenhouse). Nevertheless, a thermal influence was also detected with the calculated velocity vectors.

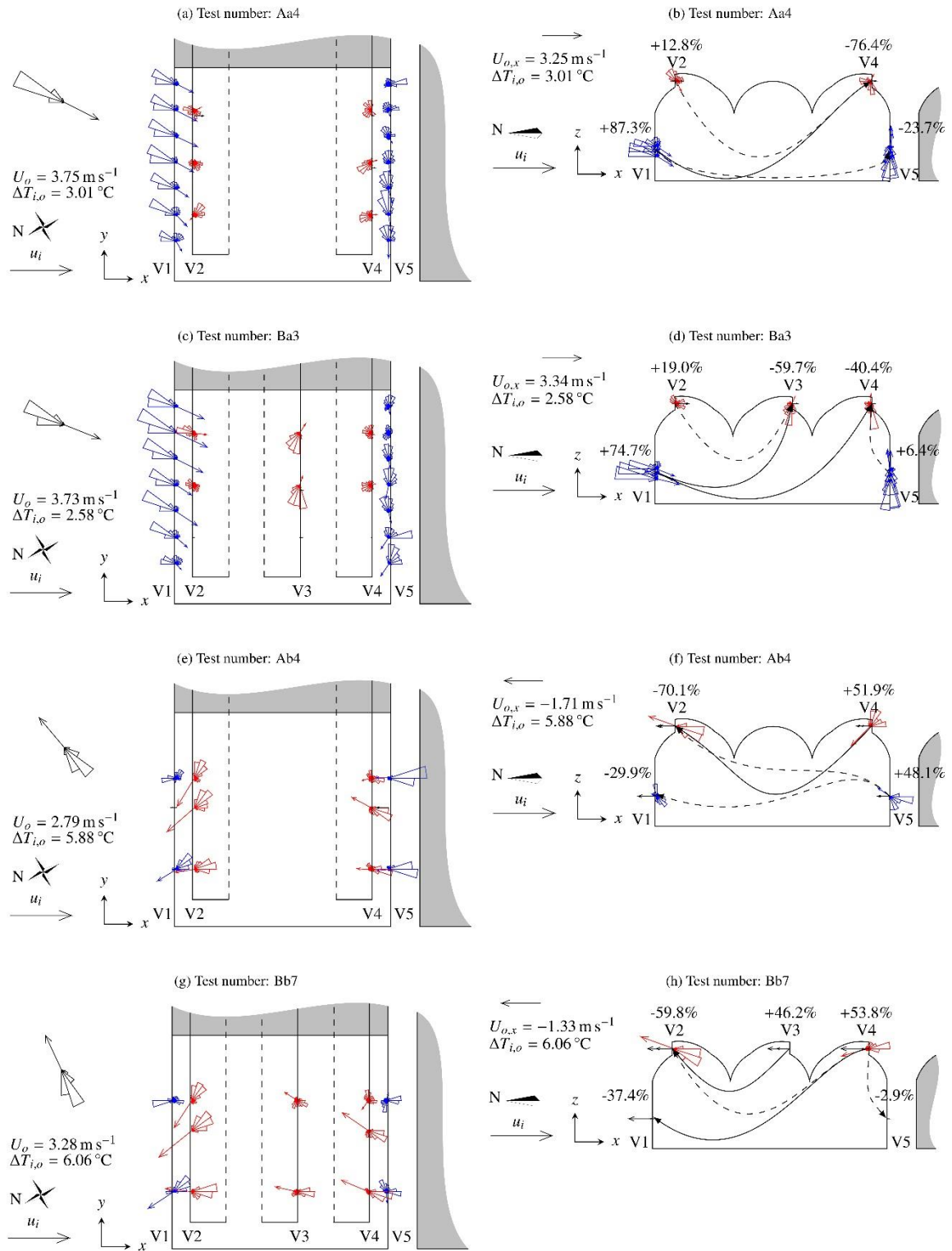





Fig. 3: Flow pattern for low wind speed from the northeast (a to d) and southwest (e to h) using setup A (a, b, e, and f) and

setup B (c, d, g, and h) in the horizontal plane XY (a, c, e, and g) and the vertical plane XZ (b, d, f, and h). Wind speed U_o and x component of the wind speed $U_{o,x}$ (the magnitude of mean wind speed vector is not represented); air temperature difference between inside and outside the greenhouse $\Delta T_{i,o}$; scale for inside flow vectors $\longrightarrow u_i = 0.5 \text{ m s}^{-1}$; mean velocity vector and polar histogram at the meteorological station , at side vents , and at roof vents ; mean flow vectors from 2D anemometers \longrightarrow ; main air stream line \longrightarrow ; and secondary air stream line $- \rightarrow$.

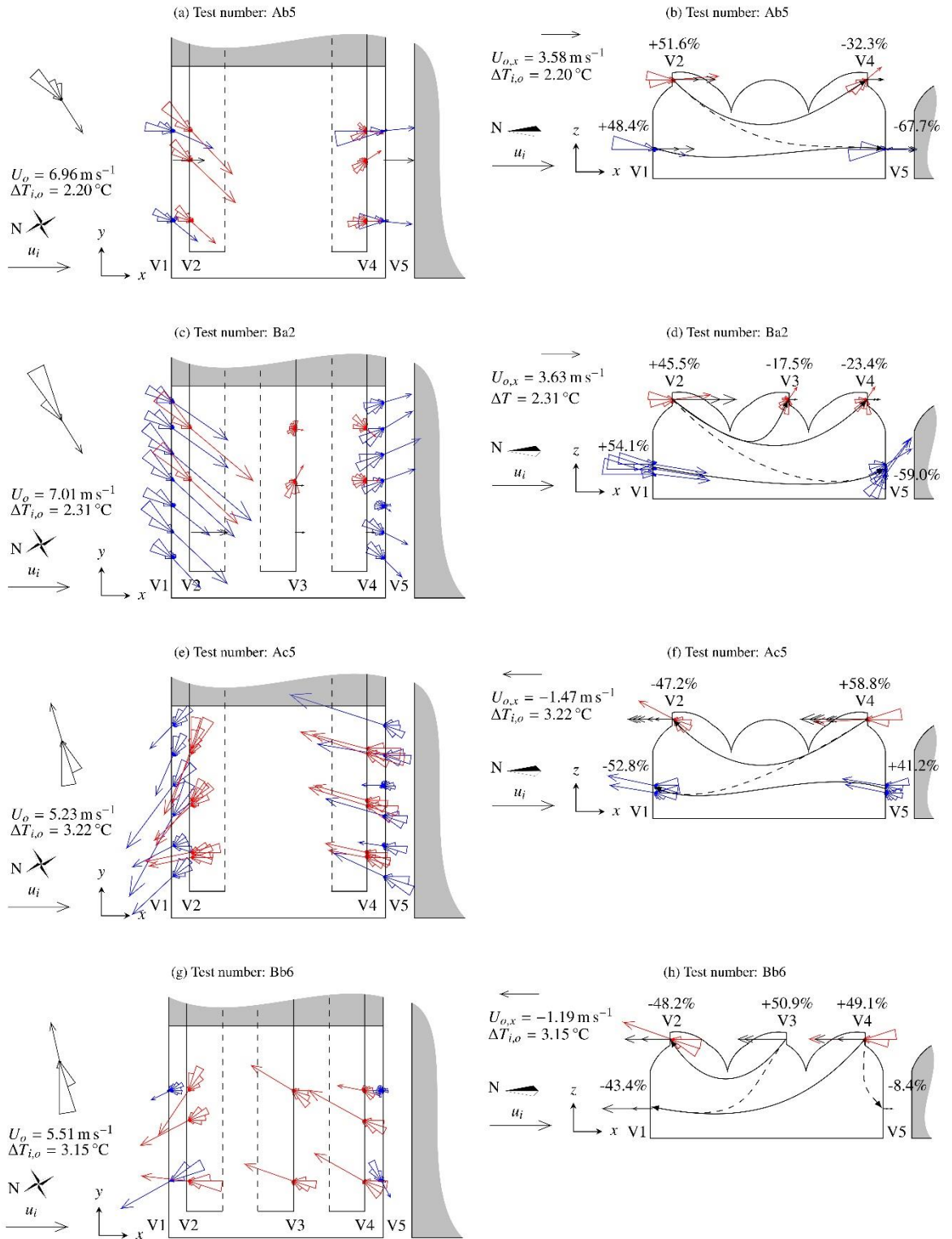





Fig. 4: Flow pattern for high wind speed from the northeast (a to d) and southwest (e to h) using setup A (a, b, e, and f) and setup B (c, d, g, and h) in the horizontal plane XY (a, c, e, and g) and the vertical plane XZ (b, d, f, and h). Wind speed U_o

and x component of the wind speed $U_{o,x}$ (the magnitude of mean wind speed vector is not represented); air temperature difference between inside and outside the greenhouse $\Delta T_{i,o}$; scale for inside flow vectors $\longrightarrow u_i = 0.5 \text{ m s}^{-1}$; mean velocity vector and polar histogram at the meteorological station , at side vents , and at roof vents ; mean flow vectors from 2D anemometers \longrightarrow ; main air stream line \longrightarrow ; and secondary air stream line $- - \blacktriangleright$.

Measured air velocity vectors field in the three-dimensional space allowed three flow patterns to be observed: a *reverse flow*, a *refracted-downward flow* and a *large horizontal eddy flow*. Due to thermal forces these flow patterns were less evident with low wind speeds than in high wind speeds where the air velocity vector direction was more disperse. A reverse flow (flow in the opposite direction to the wind) in the side vent V5 was observed in most test repetitions performed with low wind speed, except for those where $\xi < 1.33$ (supplementary material [Figs. C10b, C11b and C11f](#)) and with high wind speed when $OR > 1.00$ (supplementary material [Figs. C1a to C13b](#)). Experiments conducted by López et al. (2011), in which the same greenhouse was used but with only one open roof vent V3 and both side vents open ([Fig. 5](#)), also showed this reverse flow. Comparing the three ventilator configurations (two, three and one roof vent open, respectively) with the most similar test conditions (wind intensity and direction, and wind and thermal forces ratio), the reverse flow in vent V5 increased from 0.0% to 9.0% to 17.2% when OR_{ne} decreased from 1.00 to 0.68 to 0.51 with northeast wind ([Figs. 3b, 3d and 5a](#)). Whilst with southwest wind, the reverse flow in vent V5 increased from 0.0% to 2.9% to 33.3% when OR_{sw} increased from 1.00 to 1.48 to 1.92 ([Figs. 3f, 3h and 5b](#)). Thus, it increased when OR decreased below 1.00 for northeast wind and when OR increased above 1.00 for southwest wind. Future studies should consider evaluating the leeward obstruction when $OR_{ne} > 1.00$ and the windward obstruction when $OR_{sw} < 1.00$ to establish the effect of the obstruction in the reverse flow. However, this reverse flow also takes place when there are more spans, low windspeed and the thermal force ratio ξ .

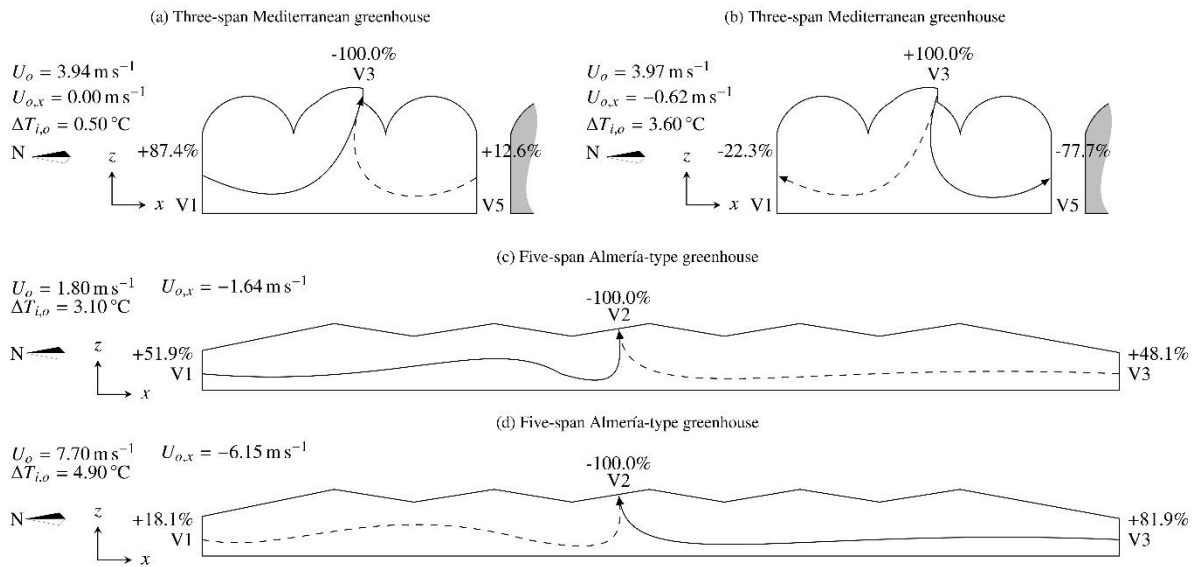


Fig. 5: Other studies results. Flow pattern in the vertical plane XZ in the same greenhouse used for this study (a and b) but configured with the middle open roof vent facing the south wind (V3) and both side vents open (V1 and V5), and an Almería greenhouse (c and d) exposed to low-speed northeast wind (a), low-speed southwest wind (b and c), and high-speed south wind (d). Wind speed U_o ; x component of the wind speed $U_{o,x}$; air temperature difference between inside and outside the greenhouse $\Delta T_{i,o}$; main air stream line \longrightarrow ; and secondary air stream line $- \longrightarrow$. Adapted from the studies developed by López (2011) (a) and Lopez et al. (2011) (b) with the same greenhouse used for this study but with one open roof vent, and from the study of Molina-Aiz et al. (2004) with a five-span Almería greenhouse (c and d).

In the experiment conducted by Molina-Aiz (2004) in a five-span Almería greenhouse, the reverse flow increased from 18.1% to 51.9% when ξ decreased from 3.48 to 1.02 (Figs. 5c and 5d respectively). With low wind speed and $\xi = 1.02$ (Fig. 5c), the reverse flow effect even became greater (51.9% of the inlet flow rate) than the inlet flow developed in the windward side vent (48.1%).

Thermal difference (and consequently density difference) between indoor and outdoor air produced a *refracted-downward* flow (observable in the vertical plane XZ) in the inlet side vent V1. This flow pattern was observed in all measurements with both low- and high-northeast windspeed components, and two and three open roof vents open (supplementary material Figs. C1g to C3d and Figs. C9a to C9f), except for measurement Ac6 (supplementary material Fig. C2d). Vents configuration did not effect this flow pattern; it was also observed in a previous study (López et al., 2012) when the greenhouse configured with one open roof vent ($U_o = 9.23 \text{ m s}^{-1}$ and $\Delta T_{i,o} = 4.00 \text{ }^\circ\text{C}$). This shows that even with the significant influence of the wind in

the velocity vectors pattern, $\Delta T_{i,o}$ affected the flow pattern at the windward side vent.

In all vents, a large horizontal eddy flow pattern was observed with the calculated air velocity vectors in the horizontal plane XY for low wind speed (Figs. 3a, 3c, 3e and 3g). When the greenhouse was ventilated with high velocity ($U_o > 5.00 \text{ m s}^{-1}$) the outlet flow direction differed from the inlet flow direction $54.8 \pm 14.5^\circ$ anticlockwise (supplementary material Figs. C1a to C13b). This flow pattern was induced by the side walls (east and west) of the greenhouse because the wind direction was not parallel to the side walls. A similar phenomenon was observed by Hong et al. (2008) in four types of naturally ventilated multi-span greenhouses when wind was 45° to the sidewall. In order to avoid this flow disturbance, greenhouse vents perpendicular to the main wind, or vents in all sidewalls of the greenhouse could be used. Teitel et al. (2015) observed a more parallel flow pattern in the interior of a screenhouse when all sidewalls were covered with the same insect-proof screen used for the roof rather than when the screenhouse was only ventilated through the roof and the sidewalls were covered with impermeable polyethylene.

3.2.2. Transition from low to high wind speeds

Flow pattern transition was defined by the threshold of the wind and thermal forces ratio ξ . Above this threshold ξ wind forces drive the flow through side vents (see ψ in Fig. 6). It was found the ξ threshold was inversely correlated to the inlet-to-outlet opening ratio OR but directly correlated to the obstruction on the leeward side. The threshold changed from $4.61 \text{ m}^\circ\text{C}^{-0.5}\text{s}^{-1}$ to $3.15 \text{ m}^\circ\text{C}^{-0.5}\text{s}^{-1}$ when OR_{ne} changed from 0.68 (setup B ventilated with northeast wind, see Fig. 6b) to 1.00 (setup A ventilated with northeast wind, see Fig. 6a). This was also observed with southwest wind; when OR_{sw} changed from 1.00 (setup A) to 1.48 (setup B) the threshold changed from $1.28 \text{ m}^\circ\text{C}^{-0.5}\text{s}^{-1}$ to $0.98 \text{ m}^\circ\text{C}^{-0.5}\text{s}^{-1}$ (see Figs. 6c and 6d, respectively). The effect of the obstruction on the reduction of the ξ threshold can be easily observed with the two open roof vents (setup A), where OR is the same in both directions ($OR_{ne,sw} = 1.00$), but the threshold was $\xi_{ne} = 3.0 \text{ m}^\circ\text{C}^{-0.5}\text{s}^{-1}$ (Fig. 6a) and $\xi_{sw} = 1.2 \text{ m}^\circ\text{C}^{-0.5}\text{s}^{-1}$ (Fig. 6c) with and without the obstruction on the leeward side, respectively. Thus, a greater wind force was needed to drive the flow through the leeward side vent when the

obstruction was on the leeward side, but also a reduction of the roof and side leeward opening surface ratio $\vartheta_{r,s}$ improved the cross-ventilation at crop level within this obstruction condition. The reduction of the threshold could be achieved by increasing the leeward side ventilation surface and reducing the leeward roof ventilation surface by means of the roof vent configuration. As was observed in the simulations of Molina-Aiz and Valera (2011), partially closed roof vents with fully opened side vents results in a better greenhouse cooling effect.

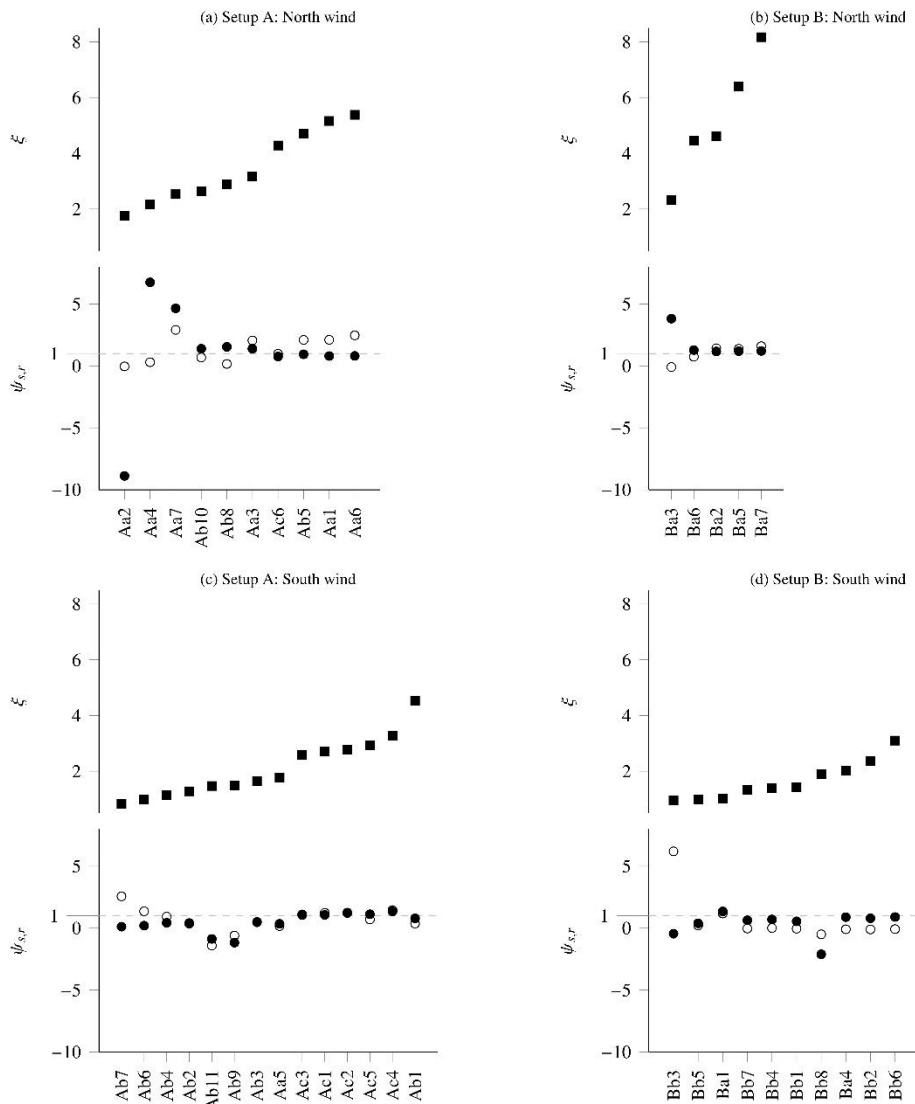


Fig. 6: Flow rate ratio between side and roof vents for the different tests carried out. By using the flow rate ratio as a descriptor, charts indicate the flow pattern transition depending of the wind and thermal forces ratio. Flow rate ratio greater than 1 indicate a greater flow through side vents than flow through roof vents. In order to observe flow rate ratio between

side and roof vent in the hole wind speed spectrum (low and high wind speed) data is ordered from low to high wind and thermal forces ratio. First row shows north wind (a and b) and second row south wind (c and d). First column shows two open roof vents (a and c) and second column shows three open roof vents (b and d). Wind and thermal forces ratio ξ (■) [$\text{m}^\circ\text{C}^{-0.5}\text{s}^{-1}$]; flow rate ratio between side and roof vents ψ : the flow rate ratio between side vent V1 and roof vent V2 $\psi_{V1,V2}$ (●) and the flow rate ratio between side vent V5 and roof vents V3 and V4 $\psi_{V5,V3,V4}$ (○).

According to Nielsen (2002); Ould Khaoua et al. (2006), the inlet flow from windward roof vents drags the air between this vent and the nearest outlet leeward roof vents, an obstacle in the ceiling of the greenhouse between the inlet and outlet vents will increase the flow rate at crop level. It can be inferred from this observation, and the measurements made at side vents, that a greater cross-ventilation at plant level was developed with setup A (Figs. 6a and 6c) when the roof and side opening ratio $\vartheta_{w,l}$ was 0.92 in both windward and leeward side. This cross-ventilation was even greater with the obstruction on the leeward side.

3.2.3. Effect of the obstruction

With the obstruction on the leeward side, the main flow was from windward side vent towards the leeward roof vents. At low wind speed, and an increase of ϑ_l from 0.92 to 1.85, in the leeward side there was a reduction in the inlet volumetric flow rate through windward side vent (Figs. 3b and 3d). As the wind and thermal forces ratio ξ increased (Fig. 6), the side-roof windward vent flow rate ratio ψ_w in both ventilator configurations tended towards 1.00. However, with high windspeed the average side-roof leeward vent flow rate ratio ψ_l was 2.18 and 1.47 for two (setup A, $OR = 1.00$) and three (setup B $OR = 0.68$) open roof vents, respectively. This means that independent of the wind speed, most of the inlet flow was shunted towards the leeward side vent when the greenhouse was configured with setup A and, hence, more air was moving at crop level. This result disagrees with that found by Kaçira, Sase and Okushima (2004b), where with an inlet-to-outlet opening ratio $OR < 1.00$ (two side vents and two leeward roof vents) higher ventilation rate was measured at the crop level than when $OR = 1.00$ (two side vents, one windward roof vent in the windward span, and one leeward roof vent in the leeward span);. However, our results agree that a greater overall volumetric flow rate is obtained when $OR < 1.00$ (using setup B) than when $OR = 1.00$ (using setup A), considering the eight test repetitions (Fig. 8).

With the obstruction to the windward side, flow tended to be from windward roof vent to leeward side vent. At low wind speed, an increase of ϑ_w from 1.00 to 1.48 (setup A and setup B, respectively) on the windward side increased the airflow rate in the leeward side vent (Figs. 3f and 3h). For high windspeed the side-roof vents flow rate ratio for windward and leeward vents ψ was close to 1.00 for setup A but in setup B this value was less than 1.00 for $\xi > 1.02 \text{ m}^\circ\text{C}^{-0.5}\text{s}^{-1}$ (Fig. 6).

Another consequence of the obstruction was a tendency for an up flow in some openings. This airflow pattern was termed the *refracted-upward* effect. In the majority of the measurements with the obstruction on the leeward side (supplementary material Figs. C1h to C3d and Figs. C8b to C9f), it was observed (in the vertical plane XZ) that flow tended to rise in all leeward vents because of the obstruction on the leeward side of the greenhouse. This flow pattern has been observed in a test performed with a low-speed north-easterly wind in a previous study with one open leeward roof vent (López et al., 2012) and in a greenhouse tunnel (Boulard et al., 2000). At low windspeeds, Tanny, Haslavsky and Teitel (2008) associated this flow pattern in the roof vent with thermal forces, whilst at high windspeeds, Perén, Van Hooff, Leite and Blocken (2016; 2015) associated this to the number of spans or the position of the leeward side vent. This flow pattern did not occur at the leeward side vent V5 in two measurements, as they were performed with wind in a parallel direction (supplementary material Figs. C1h and C2b).

The obstruction in the windward side also produced the *'refracted-upward'* effect but with $\xi > 1.48 \text{ m}^\circ\text{C}^{-0.5}\text{s}^{-1}$ for setup B (supplementary material Figs. C6d to C7h) and $\xi > 0.98 \text{ m}^\circ\text{C}^{-0.5}\text{s}^{-1}$ for setup A (supplementary material Figs. C11f and C12h). In the windward roof vents, the measured velocity vectors were parallel to the wind direction (vertical plane XZ), while velocity vectors at the windward side vent were affected by the eddy-zone already identified in a previous study (López et al., 2012).

3.3. Ventilation flow rate

The inlet flow rate G_{oi} was on average 28.2% greater than the mean flow rate G for any condition of the experiment (ventilator configuration, wind speed, and wind direction), except when the greenhouse was ventilated with a low speed southwest wind. In particular, G_{oi} was an average of $1.14G$ when the greenhouse

was configured with three open roof vents (see Fig. 8).

Comparing our results with those of other studies using different greenhouse size and ventilator configurations, some observations can be drawn (Fig. 7). When the greenhouse was ventilated at low windspeeds ($U_o < 4.00 \text{ m s}^{-1}$), the ventilation rate \bar{G}/S_g was less than that obtained by other smaller greenhouses, except those with the Almería greenhouse (Molina-Aiz and Valera, 2011) where the ventilation rate was equal or greater. When the experimental greenhouse was exposed to a high southwest wind speed ($U_o < 4.00 \text{ m s}^{-1}$), the ventilation rate was similar or greater than other greenhouses. The experimental greenhouse configured with two open roof vents barely obtained a ventilation rate of $0.04 \text{ m}^3 \text{ s}^{-1} \text{ m}^{-2}$. According to American Society of Agricultural Engineers (2003, p. 704), at this point, the ventilation has less impact in the temperature gradient inside a greenhouse.

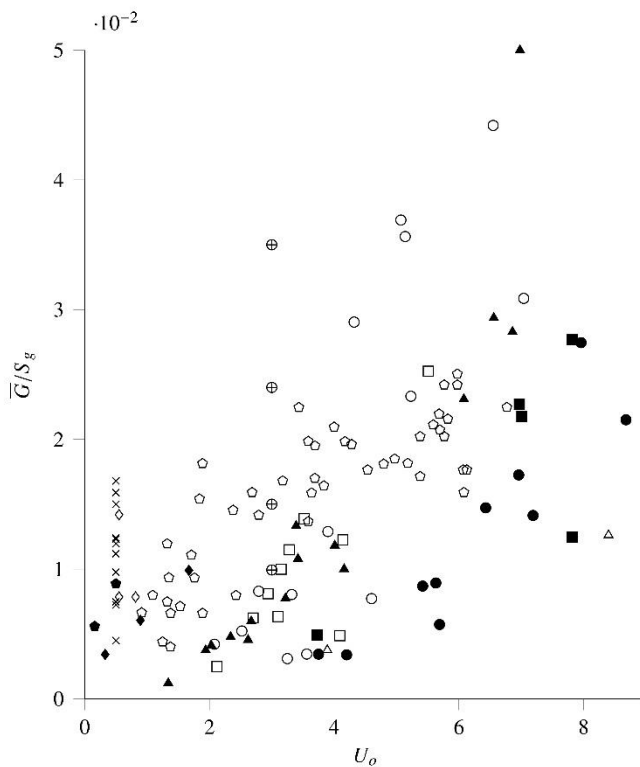


Fig. 7: Ventilation rate. Three-span Mediterranean greenhouse equipped with two open side vents and two (● and ○) and three (■ and □) open roof vents, for northeast (● and ■) and southwest wind (○ and □); Kittas, Boulard, Mermier and Papadasky (1996); greenhouse tunnel with two continuous side openings (◇); Boulard et al. (1997); Richel tunnel, Eiffel

tunnel, BN tunnel, low tunnel, Filclair plastic house, CMF glasshouse (●); Bartzanas, Boulard and Kittas (2004): one-span tunnel greenhouse with two open side vents, one open roof vent, and two open side vents and one open roof vent (⊕). Katsoulas, Bartzanas, Boulard, Mermier and Kittas (2006): one-span greenhouse with two open side vents and open roof vent (◆); Bournet, Ould Khaoua, Boulard, Migeon, and Chassériaux (2007): four-span greenhouse with one open side vent and four roof vent (✱). Teitel, Liran, Tanny, and Barak (2008): one-span greenhouse with two open side vents (⊖). López et al. (2011): three-span Mediterranean greenhouse with two open side vents and one open roof vent (▲). Molina-Aiz, Valera, and López (2011): five-span Almería greenhouse with two open side vents and two open roof vents (Δ). Ventilation rate per greenhouse floor surface G/S_g [$\text{m}^3 \text{s}^{-1} \text{m}^{-2}$] and wind speed U_o [m s^{-1}].

With high north-easterly wind speeds, the ventilation rate of the experimental greenhouse was lower than other greenhouses. In general, the resulting ventilation rates obtained in this study agreed with data measured in other studies, but not with data from studies where the effect of the vent configuration on ventilation rate was simulated using CFD (Bartzanas et al., 2004; Bournet, Ould Khaoua, Boulard, et al., 2007).

Even with the drawback that was found in the windward roof vent V2 and the leeward side vent V5, when the greenhouse was configured with three open roof vents (setup B), the mean flow rate with this configuration was 40% greater than when the greenhouse was configured with two open roof vents (supplementary material [Table A1](#)), as can be seen by comparing tests Aa4 and Ba3, which had similar wind and thermal conditions. As expected, the improvement in the ventilation surface improved the ventilation rate, in agreement with Baeza et al. (2005). However, the mean flow rate did not describe the flow in the zone between side vents occupied by the crop. The side roof vents flow rate ratio ψ , both for the windward vents and for the leeward vents, was greater when the ventilator system was configured with two open roof vents than when it was configured with three open roof vents ([Fig. 6](#)). Hence, there was a greater flow through both side vents, V1 and V5, when the greenhouse was configured with two roof vents (setup A) than when it was configured with three roof vents (setup B). This flow pattern increased the air exchange at crop level, which is important for the uniformity of the internal environmental conditions (Hong et al., 2008). Another factor that significantly affected the ventilation rate was wind orientation and the location of the obstruction. The mean flow rate was greater when the greenhouse was ventilated with south-west wind ([Fig. 8](#)) than when it was ventilated by a northeast wind. Nevertheless, no significant influence of the perpendicular component of the wind at the openings $U_{o,x}$ over the mean flow rate through the greenhouse was observed, especially when the obstruction was on the windward side. However, the average ventilation rate when the wind was parallel to the side vent

was 51.9% lower than when the wind was 23.7° to the side vent.

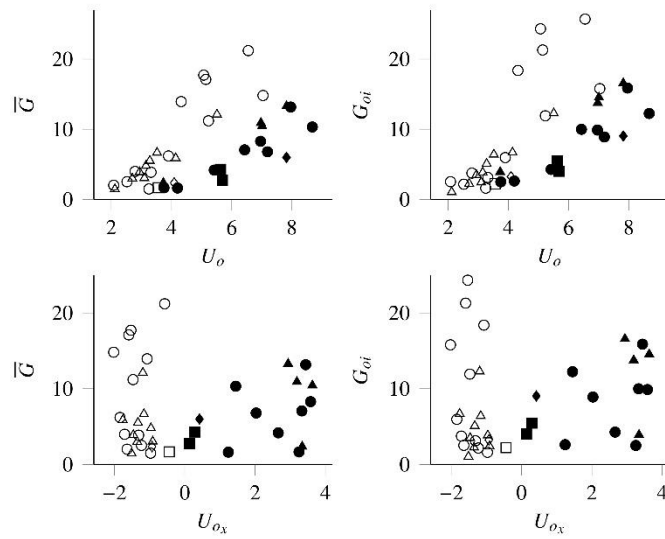


Fig. 8: Mean flow rate vs. wind speed. Mean flow rate G [$\text{m}^3 \text{s}^{-1}$]; wind speed U_o [m s^{-1}]; x component of the wind speed $U_{o,x}$ [m s^{-1}]. Setup A (●, ○, ■ and □) and Setup B (▲, △, ◆ and ◇); northeast wind (● and ▲) and southwest wind (○ and △); parallel wind from northeast (■ and ◆) and southwest (□ and ◇).

3.4. Efficiency of heat transport

The thermal energy exchange with a south west wind was always higher when the ventilating system was configured with three open roof vents (setup B) than when it was configured with two open roof vents (setup A) (see supplementary material [Table B1](#)). The average thermal energy exchange efficiency η_T was always greater for setup B. With low wind speed, η_T was 1.8 for setup B and 1.6 for setup A. For high windspeed this was similar: 1.8 for setup A and 1.9 for setup B. Nevertheless, using measuring method (c), the thermal energy exchange efficiency η_T when using setup A was 14.2% greater through the side vents than through roof vents. Thus, when comparing setup A to setup B, the resulting thermal efficiency through side vents when the greenhouse was ventilated with high speed winds from the northeast was 0.1 higher for setup A than for setup B.

4. Conclusions

The following conclusions can be drawn from the main results of the measurements of air velocity using sonic anemometry in the openings of a three-span greenhouse equipped with side and roof vents and naturally ventilated with two ventilator configurations:

Sampling method (b) was the easiest to carry out and it did not need correction of samples, but it lost spatial resolution. When sampling methodology (c) was used, which was the most difficult to carry out, a greater spatial resolution was obtained, both in terms of air velocity vectors and inlet/outlet temperature. However, a sampling reference method should be further investigated. This should take into account the difference in the normal component of the air velocity between the inlet and outlet and reduce the sample surface.

Closing one of the central roof vents changed the flow pattern inside the greenhouse, improving the air movement in the crop zone, although the overall volumetric flow rate decreased in the greenhouse. When the leeward roof vent area was reduced, the excess air entering through the windward side and roof openings exited through the leeward side opening, which improved the air flow at the crop level.

For wind speeds (U_o) less than 4 m s^{-1} and $d \xi \leq 2.3 \text{ m}^\circ\text{C}^{-0.5} \text{ s}^{-1}$, different interactions were observed between the flow rate produced by the wind (usually from the windward towards the leeward side of the greenhouse) and the flow rate produced by the buoyancy effect (from the side to the roof openings). A positive interaction was observed in the leeward roof vents and the windward side openings, and a negative interaction in the windward roof vents and the leeward side openings. Due to this negative interaction, most of the air entered through the side vent (3.7 times greater inlet flow rate than the inlet flow rate of the roof vent). While in the leeward roof openings, the positive interaction helped to remove hot air from the greenhouse. Moreover, under these conditions and when the ventilation surface of the leeward roof vents was greater than the windward roof vent surface, the leeward side opening became an entry point for air.

When wind effects prevailed over buoyancy effects (for $U_o > 4 \text{ m s}^{-1}$ and $\xi > 2.3 \text{ m}^\circ\text{C}^{-0.5}\text{s}^{-1}$), greenhouse ventilation was simplified, with air moving from the windward to the leeward openings. Under these conditions, the greenhouse obstruction controlled the airflow pattern in the greenhouse, and the flow rate through the greenhouse was reduced by the presence of the obstacle on the leeward side.

The obstruction (neighbouring greenhouse) on the leeward side reduced the ventilation capacity of the ventilation system. Nonetheless, the distribution of the ventilation surface facing the obstruction (roof and side opening surface ratio ϑ) should be considered, due to its important role in influencing the flow rate and flow pattern inside the greenhouse. Increasing ϑ worsens cross-ventilation at crop level, but it improves mean flow rate of the greenhouse.

The open roof vent configuration with the greater surface area, setup B, produced the greater thermal energy exchange efficiency η_T than setup A. Nevertheless, the surface distribution of the ventilation in setup A had a greater η_T through side vents, at crop level.

Acknowledgements

This work has been supported by the Spanish Ministry of Economy and Competitiveness and the European Regional Development Fund (ERDF) by means of the research grant AGL2015-68050-R. The authors wish to express their gratitude to the Research Centre CIAIMBITAL of the University of Almería (Spain), and the National Council of Science and Technology (CONACYT) of Mexico, for their support through the development of this study.

REFERENCES

- Álvarez, A. J., Oliva, R. M., and Valera, D. L. (2012). Software for the geometric characterisation of insect-proof screens. *Computers and Electronics in Agriculture*, 82, 134–144. <https://doi.org/10.1016/j.compag.2012.01.001>
- ASAE. (2003). *Heating, ventilating and cooling greenhouses*. USA. Retrieved from <https://elibrary.asabe.org/standards.asp>
- Baeza, E. J., Pérez-Parra, J. J., Montero, J. I., Bailey, B. J., López, J. C., and Gázquez, J. C. (2009). Analysis of the role of sidewall vents on buoyancy-driven natural ventilation in parral-type greenhouses with and without insect screens using computational fluid dynamics. *Biosystems Engineering*, 104(1), 86–96. <https://doi.org/10.1016/j.biosystemseng.2009.04.008>
- Baeza, E. J., Pérez Parra, J. J., and Montero, J. I. (2005). Effect of ventilator size on natural ventilation in parral greenhouse by means of CFD simulations. *Acta Horticulturae*, 691, 465–472. <https://doi.org/10.17660/ActaHortic.2005.691.56>
- Bartzanas, T., Boulard, T., and Kittas, C. (2002). Numerical simulation of the airflow and temperature distribution in a tunnel greenhouse equipped with insect-proof screen in the openings. *Computers and Electronics in Agriculture*, 34(1--3), 207–221. [https://doi.org/10.1016/S0168-1699\(01\)00188-0](https://doi.org/10.1016/S0168-1699(01)00188-0)
- Bartzanas, T., Boulard, T., and Kittas, C. (2004). Effect of vent arrangement on windward ventilation of a tunnel greenhouse. *Biosystems Engineering*, 88(4), 479–490. <https://doi.org/10.1016/j.biosystemseng.2003.10.006>
- Bot, G. P. A. (1983). *Greenhouse climate : from physical processes to a dynamic model*. Wageningen University & Research, Wageningen, Netherlands. Retrieved from <http://library.wur.nl/WebQuery/clc/196119#>
- Boulard, T., Feuilloley, P., and Kittas, C. (1997). Natural ventilation performance of six greenhouse and tunnel types. *Journal of Agricultural Engineering Research*, 67(4), 249–266. <https://doi.org/10.1006/jaer.1997.0167>
- Boulard, T., Kittas, C., Papadakis, G., and Mermier, M. (1998). Pressure field and airflow at the opening of a naturally ventilated greenhouse. *Journal of Agricultural Engineering Research*, 71(1), 93–102. <https://doi.org/10.1006/jaer.1998.0302>
- Boulard, T., Lamrani, M. A., Roy, J. C., Jaffrin, A., and Bouirden, L. (1998). Natural ventilation by thermal effect in a one-half scale model mono-span greenhouse. *Transactions of the American Society of Agricultural Engineers*, 41(3), 773–781. <https://doi.org/10.13031/2013.17214>
- Boulard, T., Meneses, J. F., Mermier, M., and Papadakis, G. (1996). The mechanisms involved in the natural ventilation of greenhouses. *Agricultural and Forest Meteorology*, 79(1--2), 61–77. [https://doi.org/10.1016/0168-1923\(95\)02266-X](https://doi.org/10.1016/0168-1923(95)02266-X)
- Boulard, T., Wang, S., and Haxaire, R. (2000). Mean and turbulent air flows and microclimatic patterns in an empty greenhouse tunnel. *Agricultural and Forest Meteorology*, 100(2--3), 169–181. [https://doi.org/10.1016/S0168-1923\(99\)00136-7](https://doi.org/10.1016/S0168-1923(99)00136-7)
- Bournet, P. E., and Boulard, T. (2010). Effect of ventilator configuration on the distributed climate of greenhouses: A review of experimental and CFD studies. *Computers and Electronics in Agriculture*, 74(2), 195–217. <https://doi.org/10.1016/j.compag.2010.08.007>
- Bournet, P. E., Ould Khaoua, S. A., and Boulard, T. (2007). Numerical prediction of the effect of vent arrangements on the ventilation and energy transfer in a multi-span glasshouse using a bi-band radiation model. *Biosystems Engineering*, 98(2), 224–234. <https://doi.org/10.1016/j.biosystemseng.2007.06.007>
- Bournet, P. E., Ould Khaoua, S. A., Boulard, T., Migeon, C., and Chassériaux, G. (2007). Effect of roof and side opening combinations on the ventilation of a greenhouse using computer simulation. *Transactions of the American Society of Agricultural and Biological Engineers*, 50(1), 201–212. <https://doi.org/10.13031/2013.22401>
- Campen, J. B., and Bot, G. P. A. (2003). Determination of greenhouse-specific aspects of ventilation using

- three-dimensional computational fluid dynamics. *Biosystems Engineering*, 84(1), 69–77.
[https://doi.org/10.1016/S1537-5110\(02\)00221-0](https://doi.org/10.1016/S1537-5110(02)00221-0)
- Cebeci, T. (2004). *Analysis of turbulent flows. Analysis of Turbulent Flows* (Second). Oxford: Elsevier.
<https://doi.org/10.1016/B978-008044350-8/50002-6>
- Espinoza, K., Valera, D. L., Torres, J. A., López, A., and Molina-Aiz, F. D. (2015). An auto-tuning PI control system for an open-circuit low-speed wind tunnel designed for greenhouse technology. *Sensors (Switzerland)*, 15(8). <https://doi.org/10.3390/s150819723>
- Fatnassi, H., Boulard, T., Demrati, H., Bouirden, L., and Sappe, G. (2002). Ventilation performance of a large Canarian-type greenhouse equipped with insect-proof nets. *Biosystems Engineering*, 82(1), 97–105.
<https://doi.org/10.1006/bioe.2001.0056>
- Harmanto, Tantau, H. J., and Salokhe, V. M. (2006). Microclimate and air exchange rates in greenhouses covered with different nets in the humid tropics. *Biosystems Engineering*, 94(2), 239–253.
<https://doi.org/10.1016/j.biosystemseng.2006.02.016>
- Heber, A. J., Boon, C. R., and Peugh, M. W. (1996). Air patterns and turbulence in an experimental livestock building. *Journal of Agricultural Engineering Research*, 64(3), 209–226.
<https://doi.org/10.1006/jaer.1996.0062>
- Hong, S., Lee, I., Hwang, H., Seo, I., Bitog, J. P. P., Yoo, J., ... Yoon, N. (2008). Numerical simulation of ventilation efficiencies of naturally ventilated multi-span greenhouses in Korea. *Transactions of the American Society of Agricultural and Biological Engineers*, 51(4), 1417–1432.
<https://doi.org/10.13031/2013.25235>
- Kaçıra, M., Sase, S., and Okushima, L. (2004a). Effects of side vents and span numbers on wind-induced natural ventilation of a gothic multi-span greenhouse. *Japan Agricultural Research Quarterly*, 38(4), 227–233. <https://doi.org/10.6090/jarq.38.227>
- Kaçıra, M., Sase, S., and Okushima, L. (2004b). Optimization of vent configuration by evaluating greenhouse and plant canopy ventilation rates under wind-induced ventilation. *Transactions of the American Society of Agricultural and Biological Engineers*, 47(6), 2059–2067. <https://doi.org/10.13031/2013.17803>
- Kaçıra, M., Short, T. H., and Stowell, R. R. (1998). A CFD evaluation of naturally ventilated, multi-span, sawtooth greenhouses. *Transactions of the American Society of Agricultural Engineers*, 41(3), 833–836.
<https://doi.org/10.13031/2013.17222>
- Katsoulas, N., Bartzanas, T., Boulard, T., Mermier, M., and Kittas, C. (2006). Effect of vent openings and insect screens on greenhouse ventilation. *Biosystems Engineering*, 93(4), 427–436.
<https://doi.org/10.1016/j.biosystemseng.2005.01.001>
- Katz, S. H., and Weaver, W. W. (2003). *Encyclopedia of food and culture* (Vol. 2). New York, US: Scribner. Retrieved from <http://www.worldcat.org/title/encyclopedia-of-food-and->
- Kittas, C., Boulard, T., Mermier, M., and Papadakis, G. (1996). Wind induced air exchange rates in a greenhouse tunnel with continuous side openings. *Journal of Agricultural Engineering Research*, 65(1), 37–49. <https://doi.org/10.1006/jaer.1996.0078>
- Kittas, C., Boulard, T., and Papadakis, G. (1997). Natural ventilation of a greenhouse with ridge and side openings sensitive to temperature and wind effects. *Transactions of the American Society of Agricultural Engineers*, 40(2), 415–425. <https://doi.org/10.13031/2013.21268>
- Lee, I., Sase, S., Okushima, L., Ikeguchi, A., Choi, K., and Yun, J. (2003). A wind tunnel study of natural ventilation for multi-span greenhouse scale models using two-dimensional particle image velocimetry (PIV). *Transactions of the American Society of Agricultural and Biological Engineers*, 46(3), 763–772.
<https://doi.org/10.13031/2013.13591>
- Li, Y., and Delsante, A. (2001). Natural ventilation induced by combined wind and thermal forces. *Building and Environment*, 36(1), 59–71. [https://doi.org/10.1016/S0360-1323\(99\)00070-0](https://doi.org/10.1016/S0360-1323(99)00070-0)
- López, A. (2011). *Contribución al conocimiento del microclima de los invernaderos Mediterráneos mediante*

anemometría sónica y termografía. Universidad de Almería, Almería, Spain. Retrieved from <http://cms.ual.es/UAL/estudios/doctorado/tesis/>

- López, A., Valera, D. L., and Molina-Aiz, F. D. (2011). Sonic anemometry to measure natural ventilation in greenhouses. *Sensors*, *11*(10), 9820–9838. <https://doi.org/10.3390/s111009820>
- López, A., Valera, D. L., Molina-Aiz, F. D., and Peña, A. (2011). Effects of surrounding buildings on air patterns and turbulence in two naturally ventilated Mediterranean greenhouses using tri-sonic anemometry. *Transactions of the American Society of Agricultural and Biological Engineers*, *54*(5), 1941–1950. <https://doi.org/10.13031/2013.39835>
- López, A., Valera, D. L., Molina-Aiz, F. D., and Peña, A. (2012). Sonic anemometry measurements to determine airflow patterns in multi-tunnel greenhouses. *Spanish Journal of Agricultural Research*, *10*(3), 631. <https://doi.org/10.5424/sjar/2012103-660-11>
- López, A., Valera, D. L., Molina-Aiz, F. D., Peña, A., and Marín, P. (2013). Field analysis of the deterioration after some years of use of four insect-proof screens utilized in Mediterranean greenhouses. *Spanish Journal of Agricultural Research*, *11*(4), 958–967. <https://doi.org/10.5424/sjar/2013114-4093>
- Majdoubi, H., Boulard, T., Fatnassi, H., and Bouirden, L. (2009). Airflow and microclimate patterns in a one-hectare Canary type greenhouse: An experimental and CFD assisted study. *Agricultural and Forest Meteorology*, *149*(6–7), 1050–1062. <https://doi.org/10.1016/j.agrformet.2009.01.002>
- Max, J. F. J., Horst, W. J. O., Mutwiwa, U. N., and Tantau, H. J. (2009). Effects of greenhouse cooling method on growth, fruit yield and quality of tomato (*Solanum lycopersicum* L.) in a tropical climate. *Scientia Horticulturae*, *122*(2), 179–186. <https://doi.org/10.1016/j.scienta.2009.05.007>
- Miguel, A. F., Van De Braak, N. J., and Bot, G. P. A. (1997). Analysis of the airflow characteristics of greenhouse screening materials. *Journal of Agricultural Engineering Research*, *67*(2), 105–112. <https://doi.org/10.1006/jaer.1997.0157>
- Molina-Aiz, F. D., and Valera, D. L. (2011). Configuration by evaluating ventilation efficiency based on computational fluid dynamics. *Acta Horticulturae*, *893*, 669–678. <https://doi.org/10.17660/ActaHortic.2011.893.71>
- Molina-Aiz, F. D., Valera, D. L., and Álvarez, A. J. (2004). Measurement and simulation of climate inside Almería-type greenhouses using computational fluid dynamics. *Agricultural and Forest Meteorology*, *125*(1–2), 33–51. <https://doi.org/10.1016/j.agrformet.2004.03.009>
- Molina-Aiz, F. D., Valera, D. L., Álvarez, A. J., and Madueño, A. (2006). A wind tunnel study of airflow through horticultural crops: Determination of the drag coefficient. *Biosystems Engineering*, *93*(4), 447–457. <https://doi.org/10.1016/j.biosystemseng.2006.01.016>
- Molina-Aiz, F. D., Valera, D. L., and López, A. (2011). Airflow at the openings of a naturally ventilated Almería-type greenhouse with insect-proof screens. *Acta Horticulturae*, *893*, 545–552. <https://doi.org/10.17660/ActaHortic.2011.893.56>
- Molina-Aiz, F. D., Valera, D. L., Peña, A., and Gil, J. (2005). Optimisation of Almería-type greenhouse ventilation performance with computational fluid dynamics. *Acta Horticulturae*, *691*, 433–440. <https://doi.org/10.17660/ActaHortic.2005.691.52>
- Molina-Aiz, F. D., Valera, D. L., Peña, A., Gil, J., and López, A. (2009). A study of natural ventilation in an Almería-type greenhouse with insect screens by means of tri-sonic anemometry. *Biosystems Engineering*, *104*(2), 224–242. <https://doi.org/10.1016/j.biosystemseng.2009.06.013>
- Nielsen, O. F. (2002). Natural ventilation of a greenhouse with top screen. *Biosystems Engineering*, *81*(4), 443–451. <https://doi.org/10.1006/bioe.2002.0052>
- Norton, T., Grant, J. J., Fallon, R. J., and Sun, D.-W. (2009). Assessing the ventilation effectiveness of naturally ventilated livestock buildings under wind dominated conditions using computational fluid dynamics. *Biosystems Engineering*, *103*(1), 78–99. <https://doi.org/10.1016/j.biosystemseng.2009.02.007>
- Ould-Khaoua, S. A., Bournet, P. E., Migeon, C., Boulard, T., and Chassériaux, G. (2006). Analysis of

- greenhouse ventilation efficiency based on Computational Fluid Dynamics. *Biosystems Engineering*, 95(1), 83–98. <https://doi.org/10.1016/j.biosystemseng.2006.05.004>
- Perén, J. I., Van Hooff, T., Leite, B. C. C., and Blocken, B. (2015). CFD analysis of cross-ventilation of a generic isolated building with asymmetric opening positions: Impact of roof angle and opening location. *Building and Environment*, 85, 263–276. <https://doi.org/10.1016/j.buildenv.2014.12.007>
- Perén, J. I., Van Hooff, T., Leite, B. C. C., and Blocken, B. (2016). CFD simulation of wind-driven upward cross ventilation and its enhancement in long buildings: Impact of single-span versus double-span leeward sawtooth roof and opening ratio. *Building and Environment*, 96, 142–156. <https://doi.org/10.1016/j.buildenv.2015.11.021>
- Perén, J. I., Van Hooff, T., Ramponi, R., Blocken, B., and Leite, B. C. C. (2015). Impact of roof geometry of an isolated leeward sawtooth roof building on cross-ventilation: Straight, concave, hybrid or convex? *Journal of Wind Engineering and Industrial Aerodynamics*, 145, 102–114. <https://doi.org/10.1016/j.jweia.2015.05.014>
- Roy, J. C., and Boulard, T. (2005). CFD prediction of the natural ventilation in a tunnel-type greenhouse: influence of wind direction and sensibility to turbulence models. *Acta Horticulturae*, 691, 457–464. <https://doi.org/10.17660/ActaHortic.2005.691.55>
- Shklyar, A., and Arbel, A. (2004). Numerical model of the three-dimensional isothermal flow patterns and mass fluxes in a pitched-roof greenhouse. *Journal of Wind Engineering and Industrial Aerodynamics*, 92(12), 1039–1059. <https://doi.org/10.1016/j.jweia.2004.05.008>
- Short, T. H., and Lee, I. (2002). Temperature and airflow predictions for multi-span naturally ventilated greenhouse. *Acta Horticulturae*, 578, 141–152. <https://doi.org/10.17660/ActaHortic.2002.578.16>
- Sozzi, R., and Favaron, M. (1996). Sonic anemometry and thermometry: Theoretical basis and data-processing software. *Environmental Software*, 11(4), 259–270. [https://doi.org/10.1016/S0266-9838\(96\)00046-9](https://doi.org/10.1016/S0266-9838(96)00046-9)
- Subudhi, S., Sreenivas, K. R., and Arakeri, J. H. (2013). Study of buoyant jets in natural ventilation of a model room. *International Journal of Heat and Mass Transfer*, 64, 91–97. <https://doi.org/10.1016/j.ijheatmasstransfer.2013.04.027>
- Tanny, J., Haslavsky, V., and Teitel, M. (2008). Airflow and heat flux through the vertical opening of buoyancy-induced naturally ventilated enclosures. *Energy and Buildings*, 40(4), 637–646. <https://doi.org/10.1016/j.enbuild.2007.04.020>
- Teitel, M. (2001). The effect of insect-proof screens in roof openings on greenhouse microclimate. *Agricultural and Forest Meteorology*, 110(1), 13–25. [https://doi.org/10.1016/S0168-1923\(01\)00280-5](https://doi.org/10.1016/S0168-1923(01)00280-5)
- Teitel, M., Garcia-Teruel, M., Ibanez, P. F., Tanny, J., Laufer, S., Levi, A., and Antler, A. (2015). Airflow characteristics and patterns in screenhouses covered with fine-mesh screens with either roof or roof and side ventilation. *Biosystems Engineering*, 131, 1–14. <https://doi.org/10.1016/j.biosystemseng.2014.12.010>
- Teitel, M., Liran, O., Tanny, J., and Barak, M. (2008). Wind driven ventilation of a mono-span greenhouse with a rose crop and continuous screened side vents and its effect on flow patterns and microclimate. *Biosystems Engineering*, 101(1), 111–122. <https://doi.org/10.1016/j.biosystemseng.2008.05.012>
- Teitel, M., Ziskind, G., Liran, O., Dubovsky, V., and Letan, R. (2008). Effect of wind direction on greenhouse ventilation rate, airflow patterns and temperature distributions. *Biosystems Engineering*, 101(3), 351–369. <https://doi.org/10.1016/j.biosystemseng.2008.09.004>
- Valera, D. L., Álvarez, A. J., and Molina-Aiz, F. D. (2006). Aerodynamic analysis of several insect-proof screens used in greenhouses. *Spanish Journal of Agricultural Research*, 4(4), 273–279. <https://doi.org/10.5424/sjar/2006044-204>
- Valera, D. L., Belmonte, L. J., Molina-Aiz, F. D., and López, A. (2016). *Greenhouse agriculture in Almería. A comprehensive techno-economic analysis*. Spain: Cajamar Caja Rural. Retrieved from <http://www.publicacionescajamar.es/series-tematicas/>

- Valera, D. L., Molina-Aiz, F. D., Álvarez, A. J., López, J. A., Terrés-Nícoli, J. M., and Madueño, A. (2005). Contribution to characterisation of insect-proof screens: Experimental measurements in wind tunnel and CFD simulation. *Acta Horticulturae*, 691(2), 441–448. <https://doi.org/10.17660/ActaHortic.2005.691.53>
- Van Buggenhout, S., Van Brecht, A., Eren Özcan, S., Vranken, E., Van Malcot, W., and Berckmans, D. A. (2009). Influence of sampling positions on accuracy of tracer gas measurements in ventilated spaces. *Biosystems Engineering*, 104(2), 216–223. <https://doi.org/10.1016/j.biosystemseng.2009.04.018>
- Van Overbeke, P., De Vogeleer, G., Brusselman, E., Pieters, J. G., and Demeyer, P. (2015). Development of a reference method for airflow rate measurements through rectangular vents towards application in naturally ventilated animal houses: Part 3: Application in a test facility in the open. *Computers and Electronics in Agriculture*, 115, 97–107. <https://doi.org/10.1016/j.compag.2015.05.009>
- Van Overbeke, P., De Vogeleer, G., Pieters, J. G., and Demeyer, P. (2014). Development of a reference method for airflow rate measurements through rectangular vents towards application in naturally ventilated animal houses: Part 2: Automated 3D approach. *Computers and Electronics in Agriculture*, 106, 20–30. <https://doi.org/10.1016/j.compag.2014.05.004>
- Van Overbeke, P., Pieters, J. G., De Vogeleer, G., and Demeyer, P. (2014). Development of a reference method for airflow rate measurements through rectangular vents towards application in naturally ventilated animal houses: Part 1: Manual 2D approach. *Computers and Electronics in Agriculture*, 106, 31–41. <https://doi.org/10.1016/j.compag.2014.05.005>
- Wang, S., and Deltour, J. M. (1997). Natural ventilation induced airflow patterns measured by an ultrasonic anemometer in Venlo-type greenhouse openings. *International Agricultural Engineering Journal*, 6(3–4), 185–196. Retrieved from <http://public.wsu.edu/~sjwang/AEJ-sonic-vent.pdf>
- Wang, S., and Deltour, J. M. (1999a). Airflow patterns and associated ventilation function in large-scale multi-span greenhouses. *Transactions of the American Society of Agricultural Engineers*, 42(5), 1409–1414. <https://doi.org/10.13031/2013.13304>
- Wang, S., and Deltour, J. M. (1999b). Lee-side ventilation-induced air movement in a large-scale multi-span greenhouse. *Journal of Agricultural Engineering Research*, 74(1), 103–110. <https://doi.org/10.1006/jaer.1999.0441>